GEOLOGICA CARPATHICA, 46, 6, BRATISLAVA, DECEMBER 1995
335 - 342

GOLD IN ARSENOPYRITES FROM THE PEZINOK DEPOSIT (WESTERN CARPATHIANS, SLOVAKIA)

PETER ANDRÁŠ[1], FRITZ WAGNER[2], MILAN RAGAN[1], JOSEPH FRIEDL[2], ERIC MARCOUX[3], FRANTIŠEK CAŇO[4] and GÉZA NAGY[5]

[1] Geological Institute, Slovak Academy of Sciences, Bratislava; Branch: Severná 5, 974 01 Banská Bystrica, Slovak Republic
[2] Physik-Department E 15, Technische Universität München, D-81747 Garching, Germany
[3] BRGM, Avenue de Concyr, B.P. 6009-450600 Orléans cedex 2, France
[4] Dionýz Štúr Institute of Geology, Mlynská dolina 1, 817 04 Bratislava, Slovak Republic
[5] Laboratory for Geochemical Research, Hungarian Academy of Sciences, Budaörsi út 45, H-1112 Budapest, Hungary

(Manuscript received September 22, 1994; accepted in revised form October 5, 1995)

Abstract: Two types of arsenopyrite are found in the Pezinok deposit: fine-grained gold-bearing arsenopyrite I with average gold content 110 ppm and younger coarse-grained arsenopyrite II without gold or with a low gold content (on the average 0.17 ppm). Arsenopyrite I is the most significant gold-bearing mineral in the Pezinok-Kolársky Vrch Mt. Sb-Au deposit (ICP/MS analyses by laser-beam ablation revealing gold grades at high as 378 ppm). ^{197}Au Mössbauer study of two arsenopyrite separates showed that gold is present exclusively in a chemically bound state with isomer shift values of 3.25 mm.s^{-1} and 3.62 mm.s^{-1}, respectively. The gold-bearing arsenopyrites exhibit strong zonation patterns. Generally two extreme types of growth zones with different compositional trends can be distinguished.The first zone has antimony, sulfur and arsenic contents around 0.6-1.0 wt. % and 40-41 wt. % respectively. This zone is followed by the second one, which is also strongly zoned and has arsenic and sulfur contents around 43-45 wt. % and 19-21 wt. %, respectively. Antimony contents are 0.2 wt. % within the second zone,which is considered to be the most probable carrier of chemically bound gold.

Key words: gold-bearing arsenopyrite, state of gold, "invisible" gold, ^{197}Au Mössbauer spectroscopy, chemically bound gold, ICP/MS laser-ablation, fluid inclusions.

Introduction

The Malé Karpaty is a typical Western Carpathian mountain range consisting of the major pre-Alpine (Paleozoic) crystalline base and several minor Mesozoic nappes (Plašienka et al. 1991). Cambel (1954) distinguished two volcano-sedimentary formations of Lower Paleozoic age: *a* - the Harmonia Sequence, and *b* - the underlying Pezinok-Pernek Sequence. More recent investigations (Putiš in: Maheľ 1983; Plašienka et al. 1991) distinguished four lithological units: *1* - the Pezinok Sequence (metamorphic mantle of the Bratislava Variscan granitoid Massif), *2* - the Pernek and *3* - the Harmonia Sequences (metamorphic mantles of the Modra Variscan granodiorite Massif) and *4* - the Doľany Sequence (Fig. 1). With the exception of the Doľany Sequence these sequences consist of two formations. The lower, predominantly pelitic-psammitic formation of flysh character (Silurian-Lower Devonian) gradually passes into the overlying volcano- sedimentary formation (Lower and Middle Devonian) consisting of black schists, carbonates, basalts and their tuffs and sometimes also gabbros and gabbrodiorites (Planderová & Pahr 1983; Plašienka et al. 1991; Chovan et al. 1992). The Harmonia sequences correspond to very slightly differentiated - tholeiitic basalts which were later metamorphosed (Grecula & Hovorka 1987).

According to Putiš (1987) and Plašienka et al. (1991), the sequence of the Variscan tectono-metamorphic events was the following: 1 - regional metamorphism and folding, 2 - peri-plutonic metamorphism concluded by the intrusion of the Bratislava Granite, 3 - intrusion of the Modra Granodiorite which occurred along the tectonic contact between the Pernek and Harmonia Sequence, 4 - late Hercynian tectonic displacement of the Pernek Unit towards the Pernek and Harmonia Units causing steep metamorphic foliation with steep fold axes in the region between Pezinok and Pernek.

The Sb-Au-As deposit Pezinok-Kolársky Vrch Mt. is located in the Pernek Sequence of the Malé Karpaty mountains. Mineralization is represented mostly by veins, veinlets, incrustations and nests controlled by a wide shear zone with a NW-SE direction, situated in the Pernek Sequence, consisting of amphibolites, actinolite schists, biotite gneisses, and phylites intersected by vein bodies of granitoids. The following types of ore mineralization have been identified in the deposit:

1 - a metamorphosed, primarily exhalation-sedimentary pyrit I - pyrrhotite massive stratabound mineralization of Devonian age (Cambel 1956; Polák 1956) in black shales;

2 - a hydrothermal antimony - gold mineralization (in the form of short carbonate-sulphidic veinlets, nests and incrustations).

It has been proved by Cambel & Khun (1983) that the black shales from the mineralized belt originated in time-intervals of elevated trace element supply (Au, Ag, Sb, As, Zn, Ni, Co, V, Cu, Hg, REE ...) into the sedimentary environment. These primarily high contents of metallic elements may have resulted in the accumulation of epigenetic ore deposits. Of course some share of met-

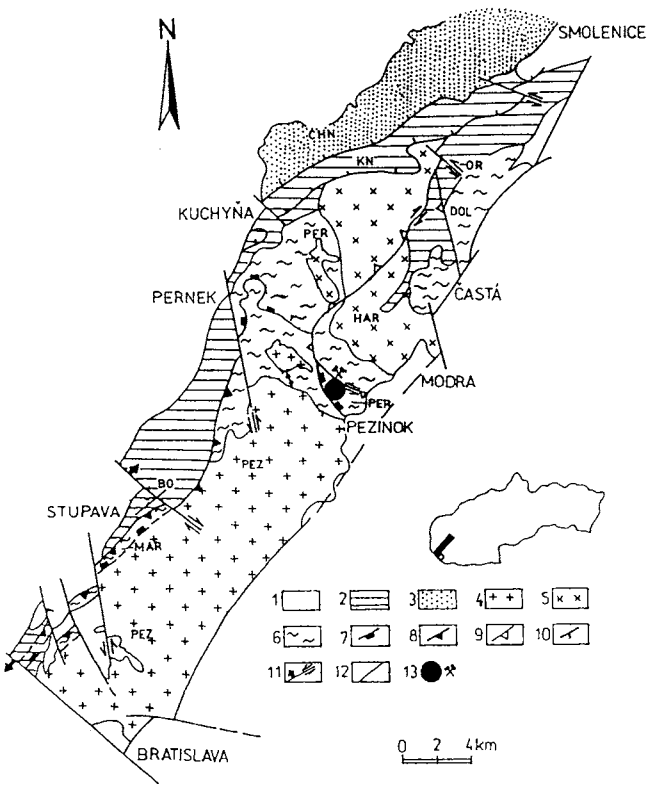

Fig. 1. Geological map of the Malé Karpaty Mts. Legend.: **PEZ**-Pezinok, **PER**-Pernek, **DOL**-Doľany, **HAR**-Harmonia sequences. **1** - Tertiary and Quarternary; **2** - Mesozoic (Triassic, Jurassic, Cretaceous); limestones, dolomites, shales, quartzites; **3** - Upper Paleozoic (Upper Carboniferous-Permian), volcano-sedimentary beds; **4** - granites of the Bratislava Massif; **5** - granodiorites of the Modra Massif; **6** - metamorphosed Paleozoic volcano-sedimentary complexes; **7** - Variscan tectonics; **8** - Alpine tectonics; **9** - Alpine overthrust faults; **10** - nappe planes; **11** - faults; **12** - geological boundaries, **13** - Pezinok mine; (after Chovan et al. 1992).

als could be mobilized by penetrating fluids not only from black schists, but also from the sedimentary sulphidic mineralization and from sedimentary-volcanic rocks (Chovan et al. 1992).

Within the epigenetic Au-As-Sb mineralization, Andráš et al. (1988, 1990) distinguished four hydrothermal periods: 1 - a quartz -arsenopyrite gold-bearing period, 2 - a quartz-pyrite-arsenopyrite period, 3 - a quartz-carbonate-stibnite period, 4 - a stibnite-kermesite period. A spatially independent quartz-gold mineralization in a small two mica granodiorite massif is younger then the first period but of unknown age in relation to the second and third periods (Cambel 1959; Andráš et al. 1988, 1990).

Two different types of arsenopyrite can be distinguished in the Pezinok deposit: *a* - the idiomorphic fine-grained arsenopyrite I, which originated in the course of the oldest first quartz-arsenopyrite hydrothermal period (Andráš 1988), and *b* - the younger coarse-grained arsenopyrite II of massive structure, crystallized from solutions of the second quartz-pyrite-arsenopyrite period (Andráš 1988).

Arsenopyrite I

The arsenopyrite I is preferentially associated with black quartz lenses or occurs in the surrounding hydrothermaly altered rocks of a shale formation in which it forms tiny impregnations of individual grains or spongy aggregates (Fig. 2) intergrown with the pyrite II, which accompanies arsenopyrite I (Fig. 3). The arsenopyrite I: pyrite II ratio varies from 10 : 1 to 3 : 1.

The arsenopyrite I forms small idiomorphic and hypidiomorphic prismatic grains, which commonly have a thickness of 0.001-0.5 mm and are exceptionally 1-2 mm long. The crystals are often tectonically fractured, exhibiting signs of corrosion at the margins (Figs. 4, 5). Various composite crystals, especially crossed composites (Fig. 6) and star triplets (Fig. 7), are characteristic. The homogenization temperature derived from fluid inclusions in quartz-bearing arsenopyrite I (and pyrite II) ranges from 140 to 275 °C (on the average 225 °C). The aqueous H_2O-NaCl fluids have low salinities from 4 to 8 equiv. wt. percent (Dubaj, unpublished data).

These data are similar to those from deposits at Villeranges (Boiron et al. 1987) and Le Chatelet (Boiron et al. 1988).

The results of electron microprobe analyses are given in Tab. 1. The chemical composition of arsenopyrite I crystals is shown on the ternary As-Fe-S phase diagram of Fig. 8a. The inhomogeneity of the arsenic content is shown in the histogram of Fig. 9a. The iron content ranges from 29 to 37 % (Fig. 10a). The average content of gold in arsenopyrite I determined spectrochemically is 110 ppm (Andráš et al. 1987).

The results given in Tab. 1 show that arsenopyrite I crystals exhibit large chemical variations in their As, Sb and S content. Backscattered electron scanning microscopy reveals strong chemical zonation, frequently with an As content increasing from the centre to the periphery of the arsenopyrite crystals (Figs. 11-14). Sb-poor zones with a relatively high content of As are frequent. The irregular (Fig. 14) and rhythmic (Figs. 11-13) zones are sharply separated from the zones with extremely high Sb (up to 1.26 wt. %) and S (21-29 wt. %) contents and with relatively low As content. As-rich zones were formed in only a minority of individual crystals (Figs. 12-13) and their aggregates (Fig. 11). The spatial relation of both zone types show that in the process of arsenopyrite I precipitation in the first place originated the Sb-rich zone. The sudden change of physical and chemical conditions caused that the crystallization followed by the As-rich zones (Figs. 11-13). In addition the backscattered electron microphotographs show that the compositional changes may be extreme over distances of 10 to 20 μm.

As a consequence of the low As content, arsenopyrite I is an n type semiconductor with a low thermoelectric power averaging $\alpha = 140$ μV/K (Andráš et al. 1988). There are important differences in the content of some trace elements in arsenopyrite I and arsenopyrite II (Tab. 3a, b). A comparison of these data indicates that only the gold-bearing arsenopyrite I is enriched in antimony, nickel and cobalt and it contains less copper, zinc and lead than arsenopyrite II.

Even in a detailed investigation by scanning electron microscopy (SEM) at high magnification no free gold has been observed in gold-bearing arsenopyrite I (Andráš et al. 1988). The absence of visible gold classifies the gold-bearing Au-As-Fe ore from the Pezinok deposit as a mineralization with refractory (invisible) gold.

Arsenopyrite II

The coarse grained arsenopyrite II is associated with black quartz, pyrite, chalkopyrite, stibnite, berthierite and löllingite (Cambel 1959) as gangue minerals. It forms small grains about

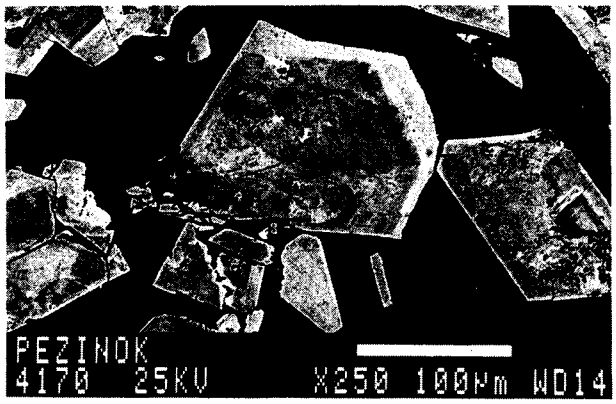

Fig. 2. Gold-bearing arsenopyrite I in quartz (black).

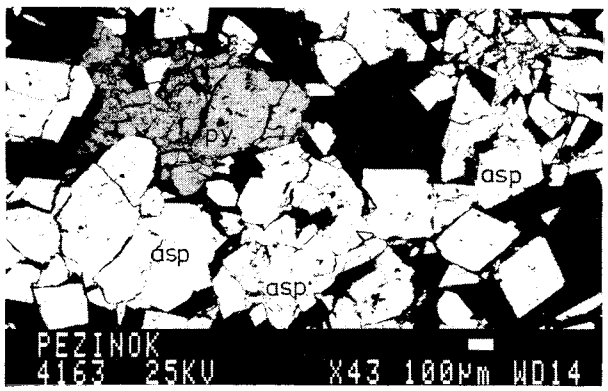

Fig. 3. Gold-bearing arsenopyrite I (**asp**) and pyrite II (**py**) in quartz (black).

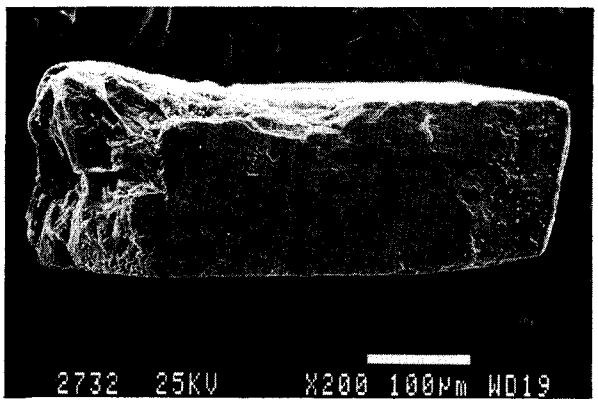

Fig. 4. Gold-bearing arsenopyrite I morphology.

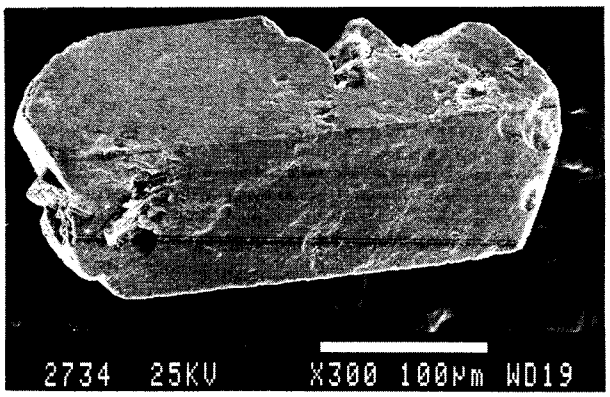

Fig. 5. Gold-bearing arsenopyrite I morphology.

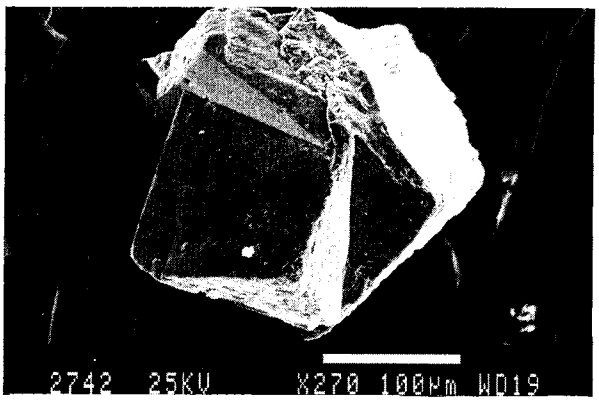

Fig. 6. Morphology of gold-bearing arsenopyrite I (twinned crystals).

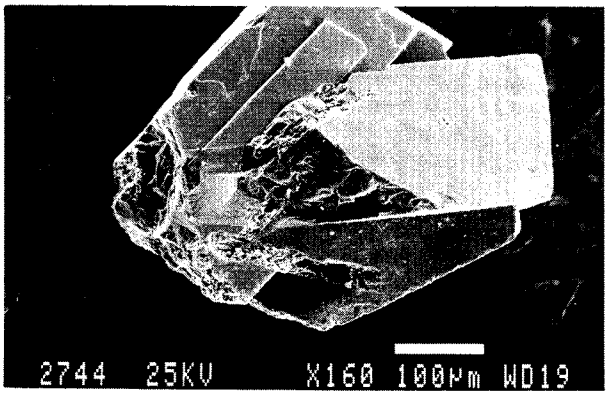

Fig. 7. Morphology of gold-bearing arsenopyrite I star triplets.

0.01-0.005 mm in size. The crystals are often tectonically fractured (Fig. 15). Arsenopyrite II differs from the older, gold-bearing arsenopyrite I in lower reflectance, in disseminated structures or brecciated massive structures and in allotrimorphic textures (Figs. 15, 16). It originates from the replacement of older pyrite or from direct precipitation from solutions during the second hydrothermal period.

The results of electron microprobe analyses of arsenopyrite II are given in Tab. 2. The chemical composition is characterizated on the ternary As-Fe-S diagram of Fig. 8b and seems to be very homogenous (Fig. 9b). The iron content ranges from 34 to 37 wt. % (Fig. 10b). The average content of gold in arsenopyrite II determined by atomic absorption with electrothermal atomisation is 0.17 ppm. Arsenopyrite II differs from arsenopyrite I in the ab-

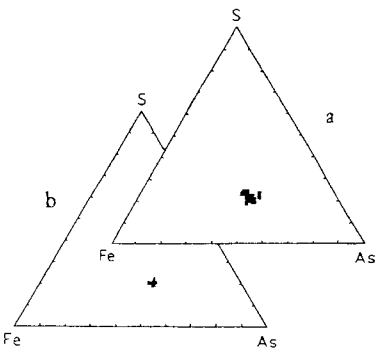

Fig. 8. As-Fe-S graph of individual electron microprobe analyses (in wt.%): **a** - of gold-bearing arsenopyrite I, **b** - of arsenopyrite II.

Table 1: Electron microprobe analyses (wt. %) of arsenopyrite I.

Sample No.	wt.%				
	Fe	As	Sb	S	Total
1	29.13	46.84	0.50	23.24	99.71
2	29.18	46.93	0.54	23.28	99.93
3	32.58	44.97	0.71	21.80	100.06
4	32.86	45.80	0.42	20.18	99.26
5	32.99	45.55	0.72	21.59	99.85
6	33.08	46.43	0.04	20.40	99.95
7	33.16	45.17	0.33	21.21	99.87
8	33.26	46.69	0.04	20.52	100.51
9	33.38	41.77	0.74	23.68	99.53
10	33.44	46.63	0.38	19.66	100.11
11	33.47	45.60	0.33	21.41	100.81
12	33.60	43.82	0.05	21.80	99.27
13	33.70	46.60	0.37	19.68	100.35
14	33.94	43.80	-	21.34	99.08
15	34.06	46.62	0.05	20.05	100.78
16	34.09	44.04	0.16	20.99	99.28
17	34.23	46.34	0.05	19.80	100.42
18	34.28	43.71	0.23	28.84	99.09
19	34.31	45.42	0.07	20.97	100.77
20	34.34	44.44	0.12	21.19	100.09
21	34.34	44.35	0.17	21.14	100.00
22	34.37	44.03	-	20.67	99.07
23	34.43	43.92	0.15	21.35	99.85
24	34.47	44.89	-	20.20	99.60
25	34.50	44.36	-	20.62	99.48
26	34.50	43.76	0.08	21.67	100.00
27	34.51	40.56	0.59	23.24	98.90
28	34.52	44.64	0.11	19.74	99.01
29	34.55	45.00	-	28.25	99.84
30	34.57	44.76	0.16	21.19	100.67
31	34.58	46.81	0.05	20.00	101.44
32	34.64	44.62	-	20.74	100.00
33	34.66	44.05	0.18	21.05	99.95
34	34.67	43.09	0.33	21.79	99.88
35	34.67	43.68	0.02	22.14	100.51
36	34.74	43.17	0.31	21.84	100.06
37	34.85	43.80	-	20.32	98.97
38	34.86	42.63	0.69	21.86	100.16
39	34.86	43.82	-	20.33	99.01
40	34.87	43.02	-	20.33	99.02
41	34.92	43.35	-	21.45	99.72
42	34.97	44.90	0.28	21.69	101.84
43	34.98	43.25	0.14	22.10	99.47
44	35.05	45.25	-	20.68	100.98
45	35.11	41.49	0.68	23.48	100.75
46	35.13	41.48	1.04	23.12	100.77
47	35.16	40.30	1.26	23.85	100.58
48	35.18	43.63	-	19.93	99.74
49	35.23	41.77	1.25	23.27	101.52
50	35.37	40.87	0.69	23.45	100.38
51	35.40	40.78	1.03	23.66	100.95
52	35.40	40.70	0.77	23.85	100.72
53	35.81	40.94	-	22.81	99.56
54	35.82	39.90	0.90	22.40	99.02
55	35.82	39.90	0.90	22.41	99.03
56	36.77	44.03	-	18.86	99.66

Table 2: Electron microprobe analyses (wt. %) of arsenopyrite II.

Sample No.	wt.%				
	Fe	As	Co	S	Total
1	33.90	46.16	0.09	20.22	100.37
2	34.04	45.07	-	21.87	100.98
3	34.19	45.70	-	20.02	99.91
4	34.27	45.53	0.10	19.84	99.74
5	34.35	45.59	-	20.32	100.26
6	34.38	45.06	-	20.84	100.28
7	34.38	45.88	-	19.70	99.99
8	34.45	45.20	0.05	20.69	100.39
9	34.48	45.40	-	20.76	100.64
10	34.58	45.85	-	20.46	100.99
11	34.67	45.82	-	20.50	100.99
12	34.68	46.20	0.06	20.05	100.99
13	34.74	45.52	-	29.62	99.89
14	34.77	45.01	0.10	20.56	100.44
15	34.81	44.64	-	20.47	99.92
16	34.89	44.83	-	20.44	100.16
17	34.95	45.29	-	20.64	100.88
18	34.96	44.35	-	20.45	99.76
19	34.99	45.32	-	20.68	100.99
20	35.01	45.01	-	20.11	100.13
21	35.14	44.87	-	20.73	100.74
22	35.18	45.09	-	20.67	100.94
23	35.18	44.63	0.06	19.93	99.80
24	35.50	45.10	-	19.59	100.20
25	35.64	45.54	-	19.35	100.53
26	36.53	43.55	-	20.11	100.19

Legend to Tables 1 and 2: Analyzed with JCXA-733 (Jeol) Superprobe, V_o = 20 kV, I = 30 nA, correction ZAF, Fe, As, Co, Sb-metallic standards, S natural sulphide standards.

Table 3a: Gravimetric analyses of Fe, As and S, flame atomic absorption spectrometry determination of Sb, Ni, Co, Cu, Bi and determination of gold by electrothermal atomisation in arsenopyrite I. Concentrations of Zn and Pb are below detection limit.

Sample No.	wt.%			ppm					
	Fe	As	S	Sb	Ni	Co	Cu	Bi	Au
1	35.43	39.80	23.48	4700	214	56	34	3	121
2	33.38	36.10	22.80	3400	256	78	54	2	75
3	32.82	39.00	22.16	6300	354	72	71	5	74
4	34.29	39.80	23.08	4100	360	110	56	4	78

Table 3b: Analysis data for arsenopyrite II: Flame atomic absorption spectrometry determination of Ni, Cr, Zn, Mn, Pb and Cu. Determination of gold by electrothermal atomisation. Concentrations of Co and Bi are below detection limit.

Sample No.	ppm						
	Au	Ni	Cr	Zn	Mn	Pb	Cu
1	0.11	20	40	360	460	80	5
2	0.05	30	3	4040	380	75	3
3	0.59	60	25	306	125	50	45
4	0.02	44	50	210	87	-	-
5	0.10	20	3	15	97	-	80

Legend to Tables 3a and 3b: All results were obtained using a single beam atomic absorption spectrophotometer Pye Unicam/ Philips, model PU-9000 with electrothermic atomiser Series PU 9095.

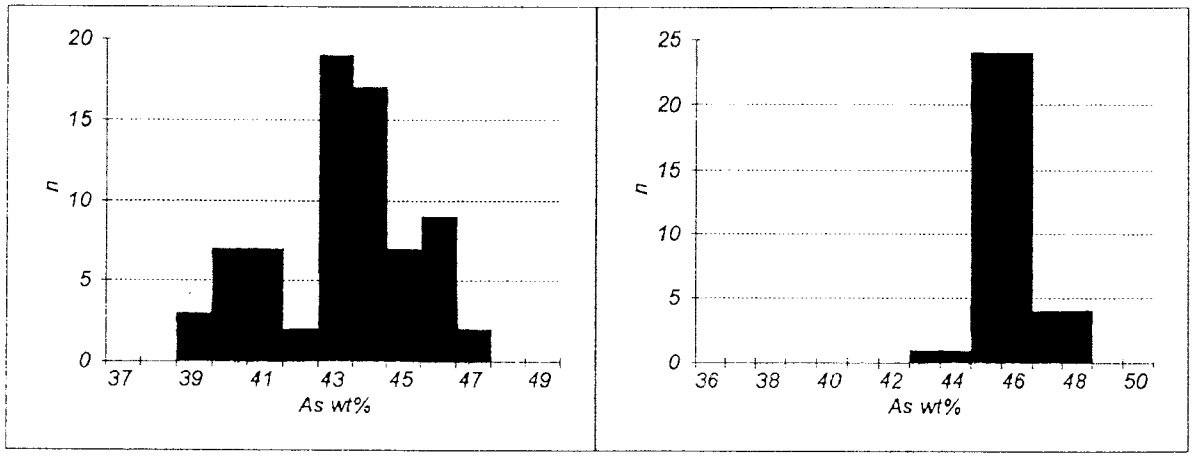

Fig. 9. As content (wt. %): **a** - in gold-bearing arsenopyrite I, **b** - in arsenopyrite II.

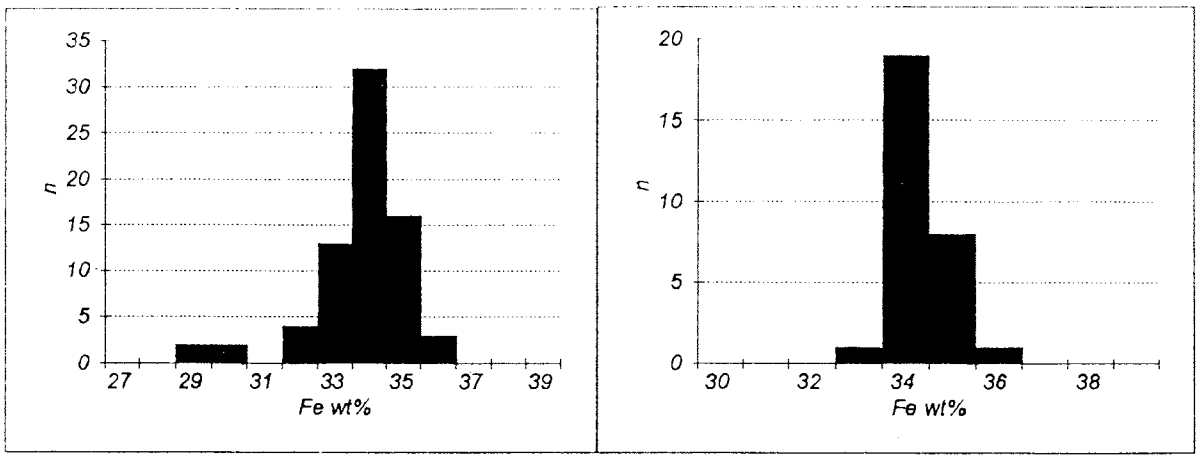

Fig. 10. Fe distribution (wt. %) **a** - in gold-bearing arsenopyrite I, **b** - in arsenopyrite II.

sence of antimony and in trace contents of cobalt up to 0.10 wt. % (Tab. 1, 2) (Andráš et al. 1987).

The homogenization temperatures of fluid inclusions in black quartz paragenetically related to arsenopyrite II range between 150 and 200 °C, and the salinities of the aqueous H_2O-NaCl fluids range from 5 to 9 equiv. wt. percent (Dubaj unpublished data).

Experimental

A ^{197}Au Mössbauer spectroscopic study of the nature of the gold in two samples of arsenopyrite I has been performed at the Technical University of Munich. This method requires the vicinity of a nuclear reactor, in order to reactivate the short lived ^{197}Pt gamma ray source with a half-life of $T_{1/2}$ = 19 hours only. The method and the determination of the Lamb-Mössbauer factors for combined gold within sulphides are described elsewhere (Wagner et al. 1986; Friedl et al. 1991).

The sources were made by neutron irradiation of about 200 mg of isotopically enriched ^{197}Pt metal in a thermal neutron flux of about 2×10^{13}/(cm^2.s^{-1}) in the Munich Research Reactor. For the Mössbauer measurements both the source and the absorber were cooled to 4.2 K in a liquid helium bath cryostat. The 77 keV gamma radiation used for ^{197}Au Mössbauer spectroscopy was detected by an inbriuric germanium detector. The spectra were least squares fitted with Voigt profiles generated by a gaussian

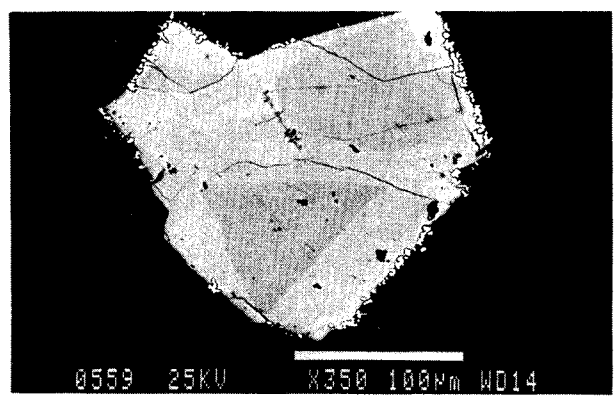

Fig. 11. Back scattered electron image of a portion of the polished section of gold-bearing arsenopyrite I aggregates with As-rich rims and Sb rich cores of the crystals.

distribution of the positions of lorentzian lines having the natural linewidth of the ^{197}Au Mössbauer resonance.

The absorbers of gold-bearing arsenopyrite were as thick as the photoelectric absorption of the 77 keV gamma permits, which is about 4 g/cm^2.

Gold distribution was investigated with the help of ICP/MS laser-ablation method, using the Cameca IMS 3F ion micro-

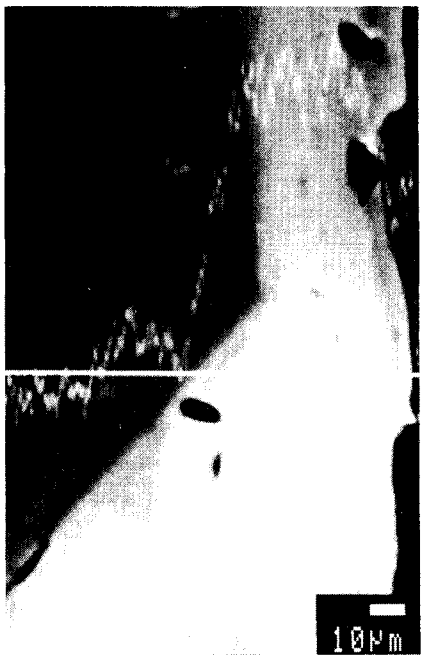

Fig. 12. Back scattered electron image of a grain of a gold-bearing arsenopyrite I crystal with an As-rich rim and line diagram of As content.

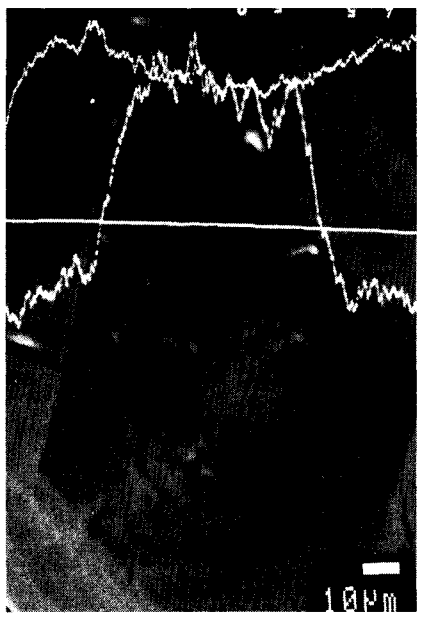

Fig. 13. Back scattered electron image of a polished section of a gold bearing arsenopyrite I crystal with line diagrams of As and Sb content.

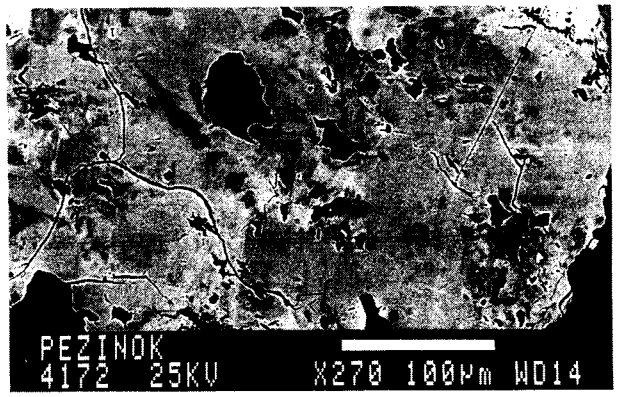

Fig. 14. Back - scattered electron image of polished section of gold-bearing arsenopyrite I with irregular composition of Sb and As distribution.

Fig. 15. Brecciated massive structure of arsenopyrite II (light-coloured) in quartz (dark).

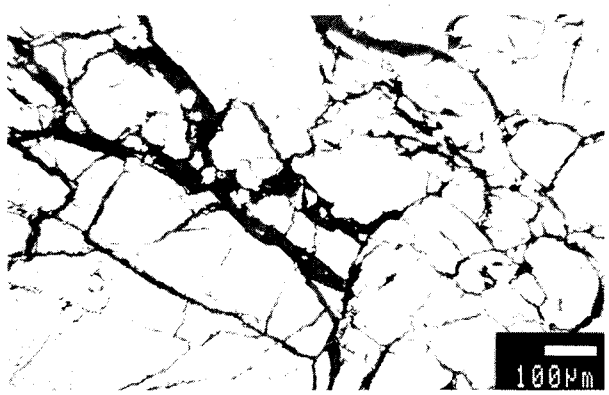

Fig. 16. Massive structure and allotriomorphic-grained texture of arsenopyrite II.

probe. Analyses were performed in the BRGM laboratories, Orléans (France). This technology enable characterization of the trace elements Au, Sb and Co within a single arsenopyrite grain at low detection limits (down to 10 ppm for gold).

Results and discussion

The mineralogical investigation ascertained that the main gold-bearing minerals on the Sb-Au-As Pezinok deposit are fine grained arsenopyrite I (in average 110 ppm Au) and pyrite

Table 4: Atomic absorption determination of Au in rims and cores of arsenopyrite I grains.

Sample No.	Analysed part of grains	Au (ppm)
1	rim	55.18
	core	0.42
2	rim	256.69
	core	22.61
3	rim	57.19
	core	15.41

Legend to Tab. 4 as in Tab. 3a, b.

Table 5a: ICP/MS laser-ablation analyses of gold-bearing small euhedral arsenopyrite I crystals from Pezinok deposit.

Sample No.	Analysed grain	ppm		
		Co	Sb	Au
RB-213	A	171	786	58
	B	51	416	378
	C	68	218	19
	D	88	116	<10
	E*	101	252	20
	E+	130	186	20
	F*	116	362	38
	F+	130	456	<10
	F+	108	398	37
	G	128	713	28
	H	88	282	30
	K*	95	823	178
	K+	79	1162	122
	L	81	256	42
	M	83	248	99
	N	91	360	22
	O	82	419	108
	P	69	157	82
	Q	54	117	17
	R	73	373	229

Table 5b: ICP/MS laser-ablation analyses of gold-bearing large euhedral arsenopyrite I crystals.

Sample No.	Analysed grain	ppm		
		Co	Sb	Au
RB-214	S++	92	1354	<10
	S+	94	1072	<10
	S*	113	2291	<10
	S**	74	1303	<10
	T^1	88	2101	48
	T^2	69	6680	84
	T^{*3}	70	4800	37
	T^{*4}	58	2927	160
	T^5	75	5302	171
	T^6	80	9204	20
	U^1	55	530	69
	U^2	58	2090	123
	U^3	65	2396	<10
	U^4	69	931	223
	U^{*5}	58	427	52
	U^{*6}	76	999	28
	Z^1	69	4137	<10
	Z^2	78	4137	<10
	Z^{*3}	67	4097	42
	Z^4	78	1872	120
	Z^5	68	1692	96

Legend to Tables 5a and 5b:
** - central part of the core;
* - core of analysed crystal;
+ - rim of analysed crystal;
++ - periphery of the rim;
A^{1-X} - analysed gradually one bottom to another

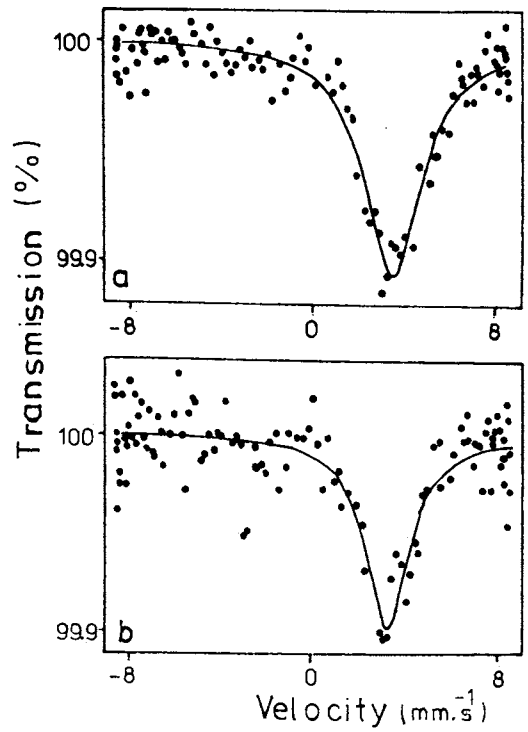

Fig. 17. Mössbauer spectra of ^{197}Au in two samples of arsenopyrite I and of a foil of mg/cm^2 of non-metallic gold: **a** - sample RB-213, **b** - sample RB-214.

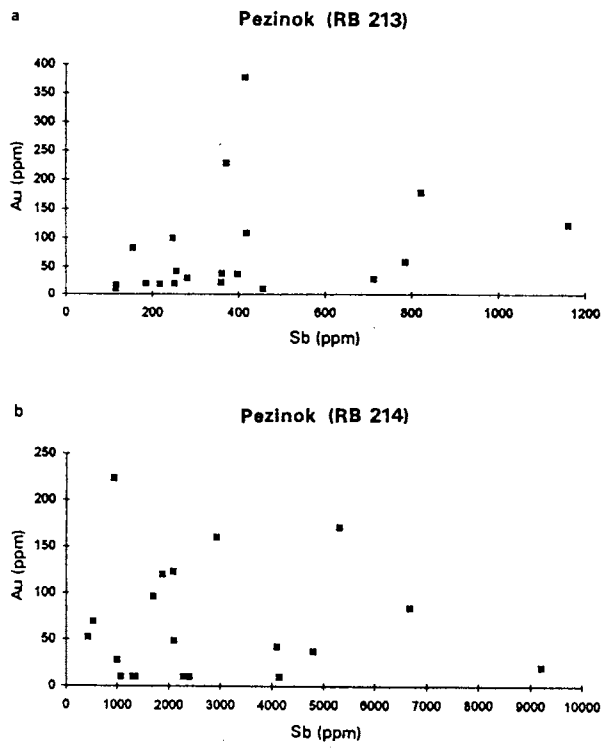

Fig. 18. Inter-element correlation between Sb and Au: **a** - in sample RB-213, **b** - in sample RB-214.

II (in average 57 ppm Au). The Au content in coarse grained arsenopyrite II is very low (in average 0.17 ppm).

Results obtained from Au-rich arsenopyrites I (sample RB-213 = 155 ppm and sample RB-214 = 80 ppm Au) show that gold is present in the samples exclusivelly as chemically bound gold which exhibits reproducible large absorption peaks at values IS ^{197}Au 3.62 mm.s^{-1} (sample RB-213) and 3.26 mm.s^{-1} (sample RB-214) (Fig. 17a, b). IS values in both samples are a little different. The reason for this diversity is the object of further investigation.

The term "invisible" gold is applied to that which occurs either as submicroscopic inclusions within the host mineral or as a solid solution or chemically bound gold thus rendering the gold refractory to conventional cyanidization. Johan et al. (1989) on the basis of relations between Au-Sb-Fe-As and S in arsenopyrites from Villeranges and Le Chatelet (France) presume Au (III) and Sb (III) together with excess of As in place of Fe atoms after scheme: 2As (Fe) → (Au, Sb) + (Fe), where As (Fe) = As on positions of Fe. Cathelineau et al. (1989) and Boiron et al. (1989) assume that the Au-As bonding is not probable but it is possible that some Au-As phase exists in arsenopyrite in from nano-inclusions.

Detailed investigation in recent years has revealed that the higher contents of gold (X00-X,000 ppm) are characteristic for fine-grained arsenopyrites of prismatic habitus. Coarse-grained aggregates of arsenopyrite only rarely contain chemically bound gold. The most convenient conditions for Au precipitation in arsenopyrite are in the time of growth of As rich zones without Sb. The growth zones of crystals with the relative highest content of Sb and S usually have the lowest content of Au (Johan et al. 1989; Marcoux et al. 1989). This assumption was confirmed by AA analyses. The margins of gold-bearing arsenopyrite I grains and their cores were dissolved separately. The results of Au determination in three samples are given in Tab. 4.

The ICP/MS laser-ablation method confirm the optical zonation of arsenopyrite I crystals. On the small crystals we could carry out only one analysis per crystal (Tab. 5a), because of the laser-beam impact (20-30 μm in diameter), but several analyses were possible across the larger crystals in sample RB-214 (Tab. 5b).

The negative inter-element correlations between Sb and Au, usually found in gold-bearing arsenopyrite, does not clearly appear (Figs. 18a, b), although there are two poorly defined trends in RB-214 sample (Fig. 18b). The supposed usual enrichment in gold around the periphery of arsenopyrite crystals (Marcoux et al. 1989) was not proved. Perhaps the size of the laser beam hinders precise mapping of any chemical zonation in small euhedral gold-bearing arsenopyrite I crystals from the Pezinok deposit.

References

Andráš P., Rajnoha J. & Hrnčárová M., 1987: Gold distribution in sulphide and non-ore minerals from the Pezinok-Kolársky vrch deposit. *Geol. Zbor. Geol. Carpath.*, 38, 5, 585-591.

Andráš P., Caňo F., Nagy G. & Durža O., 1988: Gold-bearing arsenopyrite of the Pezinok antimonite deposit. *Geol. Zbor. Geol. Carpath.*, 39, 1, 87-98.

Andráš P., Jeleň S. & Caňo F., 1990: Paragenetic relations between gold-quartz ore mineralization and antimonite ores of the Pezinok deposit, Western Slovakia. *Miner. slovaca*, 22, 429-435.

Boiron M.C., 1987: Minéralisations a Au, As, Sb altérations hydrothermales et fluides associés dans le bassin de Villeranges (Combrailles, Massif Central Francais). *Nancy Univ. Geol. Geochim. Uranium. Mem.*, 15, 1-310.

Boiron M.C., Cathelineau M., Dubessy J. & Bastoul A.M., 1988: Contrasted behaviour of Au and U in French Hercynian granites at the hydrothermal stage. The role of f_{O2} and pH. *Rc. Soc. Ital. Mineral. Petrologia Soc. mineral. ital.*, 43, 2, 485-498.

Boiron N.Ch., Cathelineau M. & Trescases J.J., 1989: Conditions of gold-bearing arsenopyrite crystallization in the Villeranges basin, Marche-Combrailles shear zone, France: A mineralogical and fluid inclusion study. *Econ. Geol.*, 84, 1340-1362.

Cambel B., 1954: Geological-petrographical problems in the northeastern part of the Malé Karpaty Mts. crystalline complex. *Geol. Práce, Zoš.*, 3, 1-538 (in Slovak).

Cambel B., 1956: Problems of the metallogeny in Malé Karpaty Mts. *Geol. Práce, Zpr.*, 9, 5-27.

Cambel B. & Kuhn M., 1983: Geochemical characteristics of black shales from ore-bearing complex of the Malé Karpaty Mts. crystalline complex. *Geol. Zbor. Geol. Carpath.*, 34, 1, 15-44.

Cambel B., 1959: Hydrothermal deposits in the Malé Karpaty Mts., mineralogy and geochemistry of their ores. *Acta geol. geogr. Univ. Comen. Geol.*, 3, 538, (in Slovak).

Cathelineau M., Boiron M. Ch., Holliger P., Marion P. & Denis M., 1989: Gold in arsenopyrites: crystal chemistry, location and state, physical and chemical conditions of deposition. *Econ. Geol. Monogr.: The geology of gold deposits*, 328-341.

Chovan M., Rojkovič I., Andráš P. & Hanas P., 1992: Ore mineralization of the Malé Karpaty Mts. (Western Carpathians). *Geol. Carpathica*, 43, 5, 275-286.

Friedl J., Wagner F.E., Sawicki J.A., Harris D.C., Mandarino J.A. & Marion Ph., 1991: ^{197}Au, ^{57}Fe, and ^{121}Sb Mössbauer study of gold minerals and ores. *Technische Univ.*, München, 1-4.

Grecula P. & Hovorka D., 1987: Early Paleosoic volcanizm of the Western Carpathians. In: Flugel H.W, Sassi F.P. & Grecula P. (Eds.): *Pre-Variscan and Variscan events in the Alpine-Mediterranean Mts. belt. Miner. slovaca, Monogr.*, 251-270.

Johan Z., Marcoux E. & Bonnemaison M., 1989: Comptes Rend 11. 308, *BRGM*, Orléans, 185.

Maheľ M., 1983: Beziehung Westkarpaten-Ostalpen, Position des Übergangs-Abschnittes-Deviner-Karpaten. *Geol. Zbor. Geol. Carpath.*, 34, 2, 131-149.

Marcoux E., Bonnemaison M., Braux Ch. & Johan Z., 1989: Distribution de Au, Sb, As et Fe dans l'arsénopyrite aurifére du Chatelet et de Villeranges (Creuse, Massif Central francais). *C. R. Acad. Sci. Paris*, Ser. II, 308, 293-300.

Putiš M., 1987: Geology and tectonics of the Malé Karpaty crystalline basement. *Miner. slovaca*. 19, 2, 135-157.

Plašienka D., Michalík J., Kováč M., Gross P. & Putiš M., 1991: Paleotectonic evolution of Malé Karpaty Mts. - an overview. *Geol. Carpathica*, 42, 4, 195-208.

Polák S., 1956: Several notes to the questions to relations between pyrite and pyrhotite of base metal minerallization in Malé Karpaty Mts. *Geol. Práce, Zpr.*, 6, 41-44.

Wagner F.E., Marion P. & Regnard J.R., 1986: Mössbauer study of the chemical state of gold in gold ores. GOLD 100. *Internat. Conf. on Gold Proc., "Extractive metallurgy of gold"*, 435-442.